

# Building Thermography: Detection of Delamination of Adhered Ceramic Claddings Using the Passive Approach

Ecem Edis · Inês Flores-Colen · Jorge De Brito

Received: 16 December 2013 / Accepted: 6 November 2014 / Published online: 18 November 2014  
© Springer Science+Business Media New York 2014

**Abstract** Tile detachment is a common durability problem of adhered ceramic claddings causing safety risks. Passive infrared thermography using solar heat gain can be used to detect delamination leading to detachment, and is advantageous especially in the inspection of middle to high-rise buildings envelope although it is qualitative by nature. In this paper, findings of in situ thermographic inspections are comparatively analysed with findings of tapping control and surface moisture measurement, and with findings of thermal simulations to evaluate their efficiency. Comparative analyses showed that passive thermography can be used as a preliminary inspection technique to detect delamination and decide whether further inspection with advanced methods is required to implement maintenance operations.

**Keywords** Passive infrared thermography · Adhered ceramic cladding · Detachment · In situ inspection · Numerical thermal simulation

## List of Symbols

$\rho$	Density (kg/m <sup>3</sup> )
$\lambda$	Thermal conductivity (W/mK)

---

E. Edis (✉)  
Faculty of Architecture, Istanbul Technical University,  
Taskisla Caddesi, Taksim, 34437 Istanbul, Turkey  
e-mail: ecem@itu.edu.tr

I. Flores-Colen · J. De Brito  
ICIST, DECivil, Instituto Superior Técnico, Universidade de Lisboa,  
Av. Rovisco Pais, 1049-001 Lisbon, Portugal  
e-mail: ines.flores.colen@ist.utl.pt

J. De Brito  
e-mail: jb@civil.ist.utl.pt

$h$	Sensible enthalpy (J/kg)
$v$	Velocity (m/s)
$T$	Temperature (°C)
$S_h$	Volumetric heat source (W/m <sup>3</sup> )
$d$	Thickness (cm)
$c$	Specific heat capacity (J/kg K)
$I_{dv}$	Diffuse solar load on vertical surface (W/m <sup>2</sup> )
$\Delta t_{[x-y]}$	Temperature difference between $x$ and $y$ (°C)
ext	External air
int	Interior air
ed	Projection of a defective area on the exterior surface
es	Sound area on the exterior surface
id	Projection of a defective area on the interior surface
is	Sound area on the interior surface

## 1 Introduction

Delamination between ceramic tiles and their substrate and the resulting detachment are among the most common durability problems observed in adhered ceramic claddings, which also give rise to safety considerations [1, 2]. Infrared thermography (IRT) is a non-destructive and remote inspection approach that can be used to detect cracks, voids, delamination problems within the component [3].

A research study was performed in Lisbon, Portugal, to discuss non-destructive inspection techniques that can be used to detect moisture and delamination problems of adhered ceramic claddings [4]. To that effect, 16 buildings were inspected by passive IRT using solar heat gain to induce observable surface temperature differences between sound and defective areas. Surface moisture device measurement and tapping control were used as alternative in situ techniques

for comparative assessment of findings when access to facade was feasible. Numerical simulations were also performed afterwards considering the inspection conditions. In relation to this research study, the detection of moisture content changes by passive approach was presented in [5].

In this paper, IRT inspections performed in two of the 16 buildings, where the presence of delamination was confirmed by tapping control, are considered. The objective is to assess the potential and efficiency of passive IRT to detect delamination problems of adhered ceramic claddings by comparatively evaluating the findings of different techniques/methods.

In IRT literature, construction-related research studies on delamination/debonding generally focus on IRT applications using artificial heat sources, and they are mainly laboratory studies, where inspections were performed in controlled environments on test samples with known characteristics [6–10]. However, especially in the case of the inspection of middle to high-rise buildings' envelopes, passive IRT is usually preferred [11, 12], as the use of artificial heating is not practical, even though it is not impossible. In addition, in the case of in situ inspections many factors such as reflections, exterior heat sources, assembly details or embedded objects may produce false or questionable thermographic indications and complicate the interpretation of thermographic findings [3, 13, 14]. Therefore, the application of passive IRT using solar heat gain in the inspection of actual buildings and the evaluation of its potential and efficiency to detect delamination problems by using alternative techniques/methods is found important, especially in terms of practical applications.

In this context, following brief theoretical data on the detection of delamination by IRT, the method and findings of numerical simulations are explained and discussed, as a base for the interpretation of IRT findings. The procedures and findings of in situ inspections are then given and discussed. Finally, all findings are evaluated to determine the potential and limits of the passive approach.

## 2 Theoretical Background

In IRT, when the inspected object is by natural causes at a different temperature than the ambient, or when natural boundary conditions cause surface temperature variations that help detect anomalies, it is called passive thermography [15, 16]. The use of solar heat gain in natural conditions is therefore considered as passive thermography in this paper.

In the detection of delamination problems by IRT, the thermal resistance of the air gap formed by the delamination helps understand the problem. In general, rather than using steady heat flow, dynamic thermal conditions are utilized to create surface temperature variations [16–18]. During heating of the surface, the surface temperature of the defective area

increases more than that of the sound area, and it continues to be higher for some time after turning off the heating source [17, 19, 20]. During the cooling period or during most of the night-time, conversely, the surface temperature of the area with delamination will be lower than that of the remaining sound area [21, 22].

## 3 Numerical Thermal Simulations

### 3.1 Computation Method

Numerical thermal simulations to understand the behaviours of sound and defective areas were performed by ANSYS 13 Fluent, a numerical fluid dynamics analysis software. The energy equation used by the software to compute the heat flux in the solid regions is as follows [23]:

$$\frac{\partial}{\partial t}(\rho h) + \nabla \cdot (\vec{v} \rho h) = \nabla \cdot (\lambda \nabla T) + S_h \quad (1)$$

In Portugal, in adhered ceramic cladding applications of frame-structured buildings, the substrate is usually hollow red clay brick infill walls and reinforced concrete structural members rendered with a cement-based undercoat. Therefore, a generic model representing three courses of hollow clay brick bonded by laying mortar, and rendered with 2 cm thick plaster on the interior side and 3 cm thick cement-based undercoat on the exterior side was used in the simulations. It was assumed that ceramic tiles were applied on the exterior surface using 2 cm thick adhesive mortar as seen in Fig. 1. In the in situ inspections, the projected sizes of areas with delamination determined by tapping control were small, and thus the thickness of the air gap might be small. Considering the delamination thicknesses used in some experimental research studies [8, 17, 21], the thickness of the air gap in the generic wall model was selected to be either 1 or 2 cm in different simulation cases to understand the effect of thickness on surface temperature variations. The air gap was designed as an enclosed air space, and only conductive heat transfer was considered during calculations. A schematic section of the generic wall model and the material properties used in the simulations are provided in Fig. 1. Three dimensional (3D) transient computations were performed on this wall model with a grid of 364,266 cells.

The hourly  $T_{\text{ext}}$  data of Lisbon was provided from the weather files of EnergyPlus energy simulation software [27], and the hourly  $I_{\text{dv}}$  data for 'fair weather conditions' was provided by using the 'solar calculator' tool of Fluent software [28], considering the dates of inspections (Fig. 2). Exterior walls inspected by IRT enveloped unconditioned interior spaces, and two different approaches were used to simulate this condition. In the first one,  $T_{\text{int}}$  was assumed to be transient, and the aforementioned hourly  $T_{\text{ext}}$  values were

**Fig. 1** Schematic section of the generic assembly model and material properties used in simulations

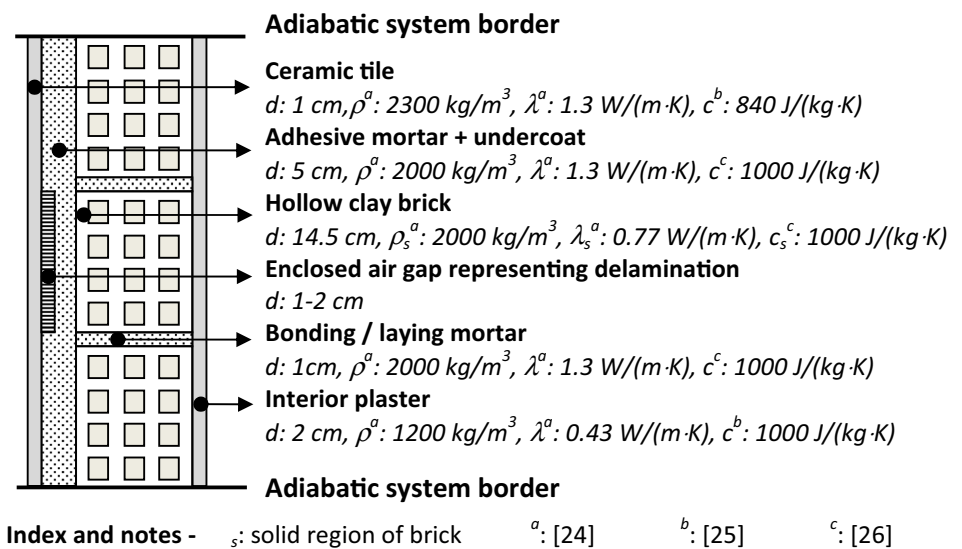
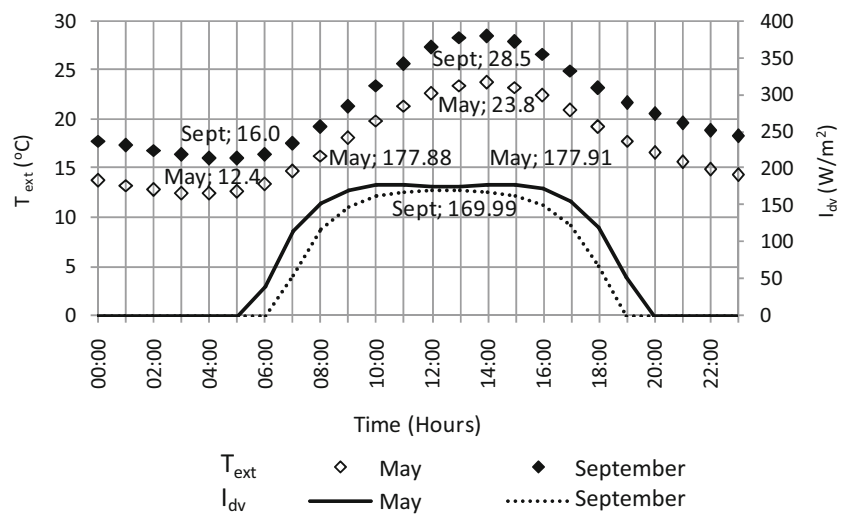


**Fig. 2** Hourly  $T_{\text{ext}}$  and  $I_{\text{dv}}$  data of Lisbon used in the thermal simulations



used for the interior space with a randomly selected time lag of 2 h. In the second approach,  $T_{\text{int}}$  was kept constant, and the arithmetical average of the hourly  $T_{\text{ext}}$  was used. As an extreme condition, a  $10^\circ\text{C}$  lower constant  $T_{\text{int}}$  than the lowest hourly  $T_{\text{ext}}$  was also used to understand whether the magnitude of the air temperature difference between external and interior spaces has an effect on the surface temperature differences observed. Thermal simulations performed and conditions defined for each simulation case are given in Table 1.

The air temperature values were defined as ‘free stream temperature (K)’ under convective thermal boundary conditions by using hourly ‘transient profiles’, and constant heat transfer coefficients of exterior and interior surfaces were defined as 25 and  $7.69 \text{ W/m}^2\text{K}$  respectively [29]. The Fluent software computed solar effects usually in relation with transparent/translucent components. Therefore,  $I_{\text{dv}}$  was

applied onto the wall model by using an assumptive heat generating wall in front of the exterior side with a thickness of 0.001 m. The hourly amount of generated heat ( $\text{W/m}^3$ ) was determined depending on the  $I_{\text{dv}}$  calculated beforehand regardless of wall orientation. The emissivity of the ceramic cladding was accepted to be 0.90 in the IRT inspections. Considering that the general emissivity (i.e. wavelength independent) and absorptivity of an opaque object have the same value as a corollary of Kirchhoff’s law, the actual amount of solar load on the exterior surface decreased according to the emissivity value.

Simulations were performed for a two-day period and the results of the second day were used in the analyses to eliminate the effect of initial conditions on the results. Two monitoring points were defined both on the external and interior sides of the generic assembly model to record the surface temperatures during the whole simulation period as given

**Table 1** Information on the thermal simulations performed

Simulation code	S1	S2	S3	S4	S5	S6	S7	S8	S9
Date considered	Ma	Ma	Ma	Ma	Ma	Se	Se	Se	Se
Solar exposure	F	F	N	N	N	F	N	F	F
$T_{\text{int}}$ condition	V	V	V	$C_A$	$C_C$	V	V	$C_A$	$C_C$
Air gap thickness (cm)	1	2	1	1	1	1	1	1	1
Associated IRT inspection	IR1	IR1	IR1, IR2	IR2	IR2	IR3	–	IR3	IR3

Ma May 27th, Se September 6th, F Fair weather, N No solar exposure, V Transient, C Constant

A Arithmetical average of hourly  $T_{\text{ext}}$

C 10 °C lower than the lowest hourly  $T_{\text{ext}}$

These abbreviations and indices are used in the text whenever necessary inside brackets following the simulation code, e.g. as S1 [MaFV1]

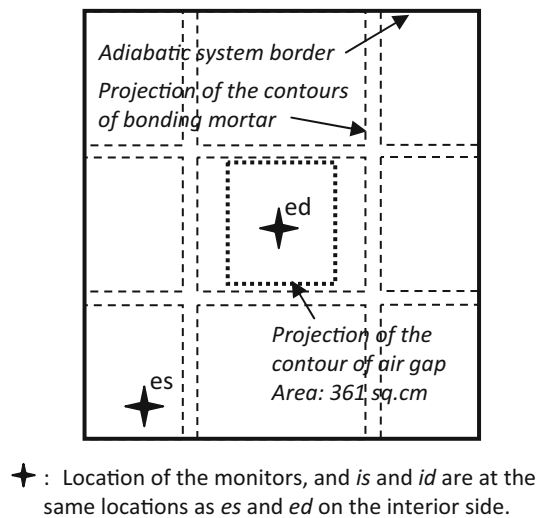


**Fig. 3** Schematic elevation of the exterior facade of the generic assembly model given in Fig. 1 and monitoring locations

in Fig. 3.  $\Delta T_{[\text{ed-es}]}$  and  $\Delta T_{[\text{id-is}]}$  were mainly used in the analyses.

### 3.2 Simulation Results

The analysis of simulation results showed that, during most of the daytime hours, when there was convective and/or solar heat gain,  $T_{\text{ed}}$  was higher than  $T_{\text{es}}$ , while the opposite occurred during the night-time hours and 1–3 h close to the sunset (Table 2, Fig. 4). The temperature distributions at the wall sections crossing the air gap showed that, during heat gain, the air gap acted as thermal insulation and delayed the heat gain of the substrate behind it as shown in Fig. 5 for simulation S9 as an example. Therefore, the temperature of the ceramic tile in front of the air gap increased consequently compared to that of the cladding in the sound area. During the heat loss of the wall, the air gap again acted as thermal insulation, but in this case delayed the heat loss of the substrate. Therefore, the temperature of the ceramic tile in front

of the air gap decreased compared to that of the cladding in the sound area. In some experimental studies [17, 19–22], similar observations were also reported in association with being in either the heating or the cooling period.

Comparative assessment of simulations S1, S3, S6 and S7, representing conditions of May and September with and without solar heat gain, revealed that solar heat gain increased the maximum and minimum  $\Delta T_{[\text{ed-es}]}$  values observed during daytime and night-time hours respectively (Fig. 4, Table 2). Similarly, a general correlation between the amount of solar load and maximum thermal contrast was also reported in an experimental study [22] for the daytime observations. In addition,  $\Delta T_{[\text{id-is}]}$  was insignificant when compared to  $\Delta T_{[\text{ed-es}]}$ , even when there was solar heat gain, which was in line with the suggestion given in [17] to perform the inspections from the side close to the defect.

The results of simulations S1 and S2 showed that the maximum and minimum  $\Delta T_{[\text{ed-es}]}$  values increased, as the thickness of the air gap increased (Fig. 6, Table 2), similarly to the experimental results reported in [21]. The size of the projected area of the defect on the surface was also reported as another determinant of  $\Delta T_{[\text{ed-es}]}$  in some experimental studies [17, 21]. Temperature distributions at the exterior side, as given for simulation S9 as an example (Fig. 4), showed gradual temperature increases or decreases at the projected location of the air gap, and also where substrate materials changed. As the greatest temperature variation was observed in the centre of the air gap, the smaller the projected area of the air gap, the smaller the temperature variation at the centre will be.

Simulation results additionally presented that, as the  $\Delta T_{[\text{ext-int}]}$  increased, the maximum and minimum  $\Delta T_{[\text{ed-es}]}$  and the time period when  $T_{\text{ed}}$  was higher than  $T_{\text{es}}$  increased (S4 vs. S5, and S8 vs. S9 in Table 2). Furthermore, the  $\Delta T_{[\text{ed-es}]}$  of each simulation was observed to reach its maximum before the heat gain of the wall ended. Then it started decreasing and reached its minimum again before the heat loss of the wall was completed (Table 2).

**Table 2** Maximum and minimum  $T_{ed}$ ,  $T_{es}$ , and  $\Delta T_{[ed-es]}$  results of simulations and their times of occurrence

Code	$T_{ed}$		$T_{es}$		$\Delta T_{[ed-es]}$		Tr. hour - → + + → -	$\Delta T_{[ed-es]}$ during IRT <sup>a</sup> Max (°C) Min (°C)
	Max (°C)	Hour <sup>b</sup>	Max (°C)	Hour <sup>b</sup>	Max (°C)	Hour <sup>b</sup>		
	Min (°C)		Min (°C)		Min (°C)			
S1	29.46	14:00	27.88	15:00	2.65	10:00	5:40	-1.88
	12.76	3:50	13.44	4:50	-2.58	20:00	17:00	-2.58
S2	29.70	14:00	27.88	15:00	2.93	10:00	5:40	-2.11
	12.64	4:00	13.44	4:50	-2.82	20:00	17:00	-2.82
S3	23.23	14:00	22.07	15:00	1.72	11:10	6:10	1.72 (-1.16)
	12.70	3:50	13.28	4:50	-1.22	20:50	16:40	1.54 (-1.22)
S4	23.27	14:00	22.17	14:50	1.61	11:10	6:20	1.59
	12.68	3:50	13.26	4:50	-1.12	20:50	16:40	1.13
S5	23.03	14:00	21.36	14:50	2.19	11:10	4:30	2.17
	12.44	3:50	12.45	4:50	-0.54	20:40	17:50	1.71
S6	33.00	14:00	31.88	14:50	3.00	11:00	6:20	-1.68
	16.33	5:00	17.00	5:20	-2.50	19:10	16:30	-2.22
S7	27.87	14:00	26.51	14:50	2.11	11:50	6:50	-1.08 <sup>c</sup>
	16.29	4:50	16.92	5:20	-1.24	21:00	16:30	-1.23 <sup>c</sup>
S8	33.81	14:00	32.02	14:50	2.88	10:50	6:30	-1.82
	16.32	4:50	17.02	5:20	-2.44	19:00	16:30	-2.44
S9	33.57	14:00	31.19	14:50	3.47	10:50	5:30	-1.23
	16.07	5:00	16.19	5:20	-1.85	19:00	17:10	-1.85

Abbreviation Tr. hour: Transition hour of  $\Delta T_{[ed-es]}$  from negative to positive, and positive to negative

<sup>a</sup>  $\Delta T_{[ed-es]}$  calculated at the simulations for the time period close to the in situ IRT inspections, which is between 19:00 and 21:00 for simulations S1, S2, and S6–S9, between 9:00 and 11:00 for simulations S4, S5, and between 9:00–11:00, and 19:00–21:00 for simulation S3, where the latter ones given in parentheses;

<sup>b</sup> Times of occurrences are approximate given in a 10 min interval;

<sup>c</sup> Simulation S7 [NV1] was a supplementary simulation where the external environmental conditions of the associated in situ thermographic inspection were not accurately modelled

## 4 In Situ IRT Inspection of Adhered Ceramic Claddings

### 4.1 Methods and Procedures

In IRT inspections, the use of solar heat gain as the driving force creating surface temperature variations was preferred mainly to detect moisture content variations of glazed ceramic tiles [5]. The use of solar heat gain also allowed detecting delamination problems during the same inspection since it created dynamic thermal conditions. In the inspections, a FLIR ThermaCAM B2 type IR camera with a spectral range of 7.5–13 μm, thermal sensitivity (NETD) of 0.1 °C and field of view (FOV) of 33.8° was used. Exterior air temperature and humidity were measured with Rothronic Hydrolog-D and HydroClip SC05. To make a comparative assessment, relative surface moisture measurements and tapping control with a rubber head hammer were performed. In the surface moisture measurements, Tramex—Survey Encounter, a capacitive type moisture measuring device, was used. The relative moisture content either at the centre or at the ends of each tile was measured, and surface moisture

maps of the areas of interest were generated with a gradual change on the surface between the measured values. In the tapping control, the presence of any delamination was checked at the corners and at the centre of each tile.

IRT inspections were usually performed in the late-afternoon or evening of a sunny day to allow proper solar heat gain and to prevent the effect of sun on thermographic inspection. Additionally, daytime inspections without any solar heat gain were also performed to analyse the effect of inspection conditions on the thermographic indications observed. Information on the conditions during the inspection of two buildings considered in this paper, namely buildings B-16 and B-11, is given in Table 3.

### 4.2 In Situ Inspection Results and Discussion

#### 4.2.1 Building B-16

In the west facade of building B-16, IRT indications of both surface temperature increase and decrease were observed in one area of interest during IR1 (Fig. 7a). Tapping control



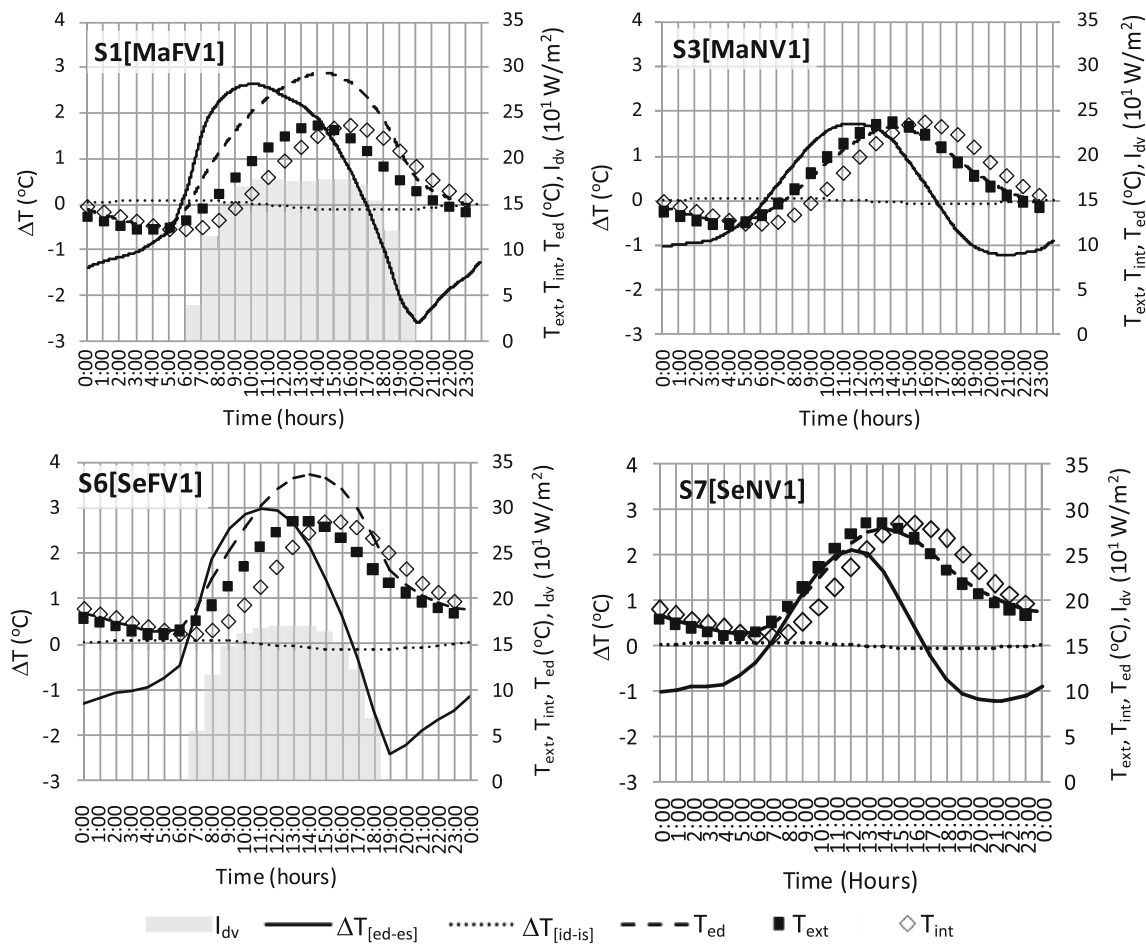


**Fig. 4** Hourly  $\Delta T_{[ed-es]}$ ,  $\Delta T_{[id-is]}$  and  $T_{ed}$  results of thermal simulations S1, S3, S6 and S7

performed in that area indicated that there were tiles with delamination where surface temperature decrease was observed, as shown in Fig. 7b. In this figure and in the following ones, a rectangle with dashed line is used whenever necessary to indicate the contour of associated area of interest. Moisture contents of some tiles with delamination were also higher than that of others, as shown in the same figure. However, IRT indication of surface temperature decrease was not linked to the moisture content increase, as higher moisture content coincided with higher surface temperature during the same inspection [5].

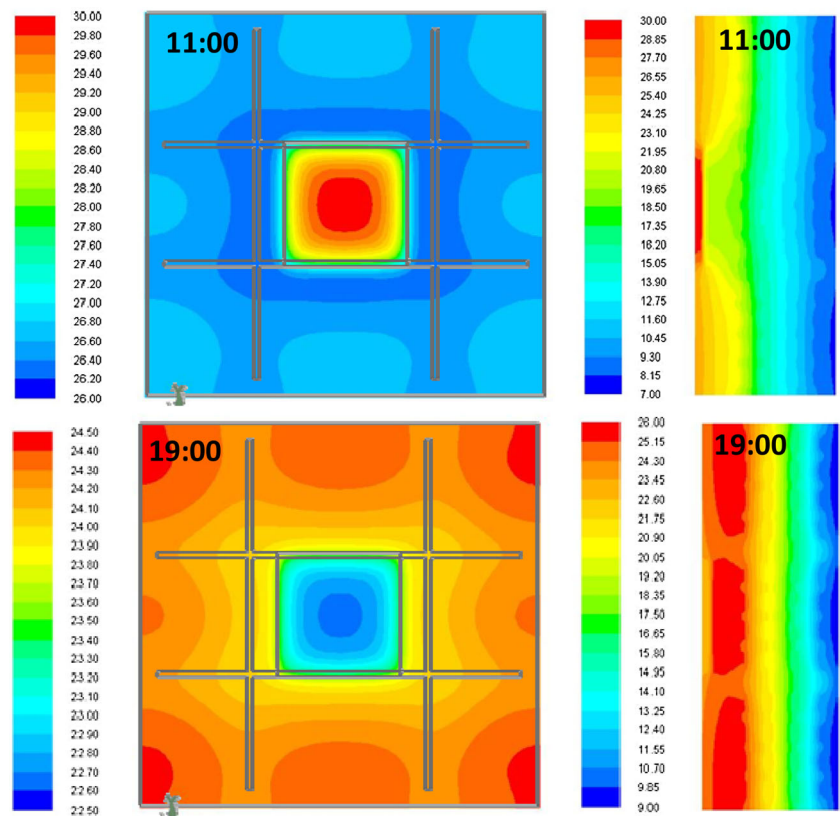
Thermogram of evening-time inspection (Fig. 8) showed that temperature decrease reaching up to 0.4 °C was present in most of the tiles with delamination, as analysed with the temperature profile line Li2. In this thermogram, and in the following ones, the label of each profile line indicates its starting point, which is on the left side of its temperature profile graph. Surface temperature increases observed close to the ground level and at the location marked with the cursor on the profile line Li1, which is the ‘+’ sign on the line, were caused by increased moisture content as discussed in [5].

Thermogram of the morning-time inspection before solar heat gain (Fig. 9), a surface temperature increase of 0.3–0.4 °C occurred at the location of the tiles with delamination, as analysed with the profile line Li2. Tiles close to the ground level and tiles marked with the cursor on the profile line Li1, both of which had higher moisture contents, also had higher surface temperature [5].

Comparison of thermograms with the tapping control results showed that thermal indications were present in the thermograms for most of the tiles with delamination (70%). In addition, comparison with the results of simulations S1–S5 verified the type of thermal indication observed in the thermograms, which was a decrease at the defective area during the evening-time inspection, while the opposite occurred in the morning-time inspection.

In simulation S1 with solar heat gain,  $\Delta T_{[es-ed]}$  calculated for a 1 cm thick air gap with a projected area on the surface similar to the actual defect was  $-(1.88-2.58)^\circ\text{C}$  for the hours close to the actual evening time inspection (Table 2). In simulation S3 without solar heat gain,  $\Delta t_{[es-ed]}$  was calculated as 1.72–1.54 °C in the hours close to the

**Fig. 5** Temperature distribution at the exterior surface and wall section crossing the air gap at hours close to when maximum and minimum  $\Delta T_{[es-ed]}$  values were calculated for simulation S9



*Grey lines indicate the contours of the bricks and the air gap.*

morning-time inspection. In the IRT inspections,  $\Delta T_{[es-ed]}$  was approximately  $-0.4^{\circ}\text{C}$  in the evening, and  $0.3-0.4^{\circ}\text{C}$  in the morning-time. Therefore, it can be said that the thickness of the air gap formed by the delamination was smaller than 1 cm, even though estimating the thickness of delamination observed is not within the scope of this paper. Similarly, in areas with delamination but without any significant surface temperature variation, the reason can be assumed to be mainly the decreased thickness of the air gap and/or its increased depth, as considered in Sect. 3.2.

#### 4.2.2 Building B-11

At the south facade of building B-11, surface temperature variations were observed in two areas of interest; namely A and B, during IR3 performed in the early evening hours (Fig. 10).

In area A, surface temperature decreases reaching up to  $0.9^{\circ}\text{C}$  were observed at the tiles close to the door frame (Fig. 11). However, no significant sound differences indicating delamination were observed by tapping the tiles where a surface temperature decrease occurred. The moisture content of tiles within that area of interest was found to range between 61 and 90 % as seen in the same figure with a moisture map based on readings at the centres of the tiles. However, no

apparent relationship between the variations of surface temperature and moisture content could be observed. During the visual inspection, loss of grout of some tiles and signs of efflorescence on the tile surfaces were observed, but the locations of the surface temperature decreases did not match the locations of those. Changes in the properties of any substrate material (e.g. its density and thus its thermal conductivity) or any material change of substrate may affect the surface temperatures observed [12,14,30]. Therefore, changes in the compactness of the adhesive mortar close to the joints or the presence of crypto-efflorescence, given the signs of efflorescence/carbonation on tile surfaces, can be assumed to be the reason for the surface temperature difference. However, it was not possible to check this assumption, since it required destructive testing (e.g. samples collection for laboratory analysis) that was not within the scope of this research study.

In area B, surface temperature decreases were observed at various locations (Fig. 12). As analysed with profile lines Li1 and Li2 as an example, these temperature decreases ranged from  $0.5$  to  $1.3^{\circ}\text{C}$ . Comparison with the tapping control results revealed that in most of the locations with delamination (78 %) a surface temperature decrease was present (Fig. 13a). On the other hand, comparison with surface moisture readings did not show such a relationship apart from 3–4

**Fig. 6** Hourly  $\Delta T_{[ed-ed]}$  results of thermal simulations

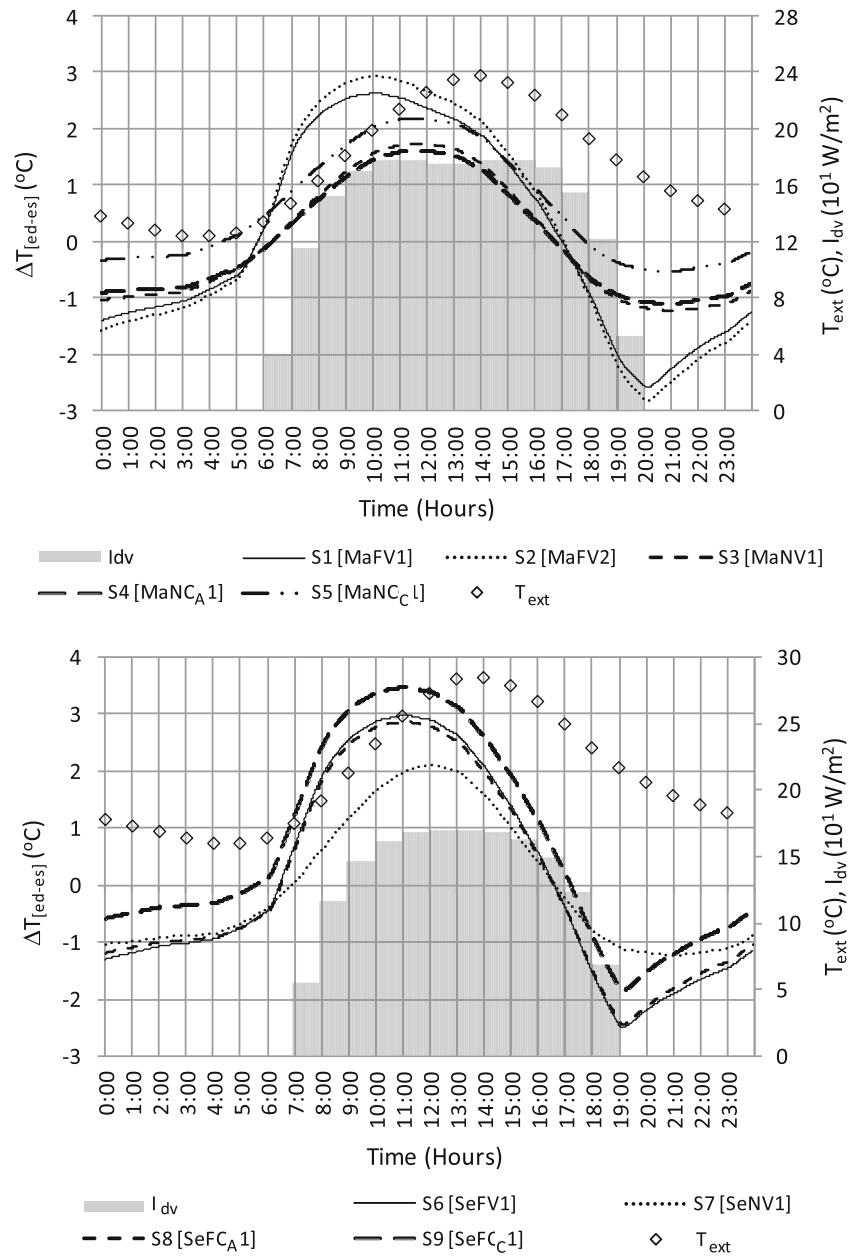


**Table 3** Information on the inspected buildings and inspection conditions

Building code	Facade orientation	Inspection date and time	Inspection code	$T_{ext}$ during inspection ( $^\circ C$ )	Predicted $T_{ext}$ (min., max.)* ( $^\circ C$ )
B-16	West	May 27th, 2010 20:00	IR1	21.4	14, 22
		May 28th, 2010 9:45	IR2	19.4	15, 22
B-11	South	September 6th, 2010 19:50	IR3	24.7	19, 29

\* Weather forecast data of National Meteorology Institute of Portugal (IM-IP)

tiles, and in those tiles the moisture contents were lower than those of others (Fig. 13b).

Simulations S6–S9 performed to analyse the case of B-16, similarly to the case of B-11, showed that an area with delamination will have lower surface temperature than its surround-

ings during evening-time inspection (Table 2). In addition, the range of  $\Delta T_{[es-ed]}$  calculated for the hours close to the actual inspection was  $-(1.23-2.44)$  for a 1 cm thick air gap. As the range of  $\Delta T_{[es-ed]}$  values observed in the thermogram of area B was  $-(0.5-1.3)^\circ C$ , the thicknesses of the air gaps



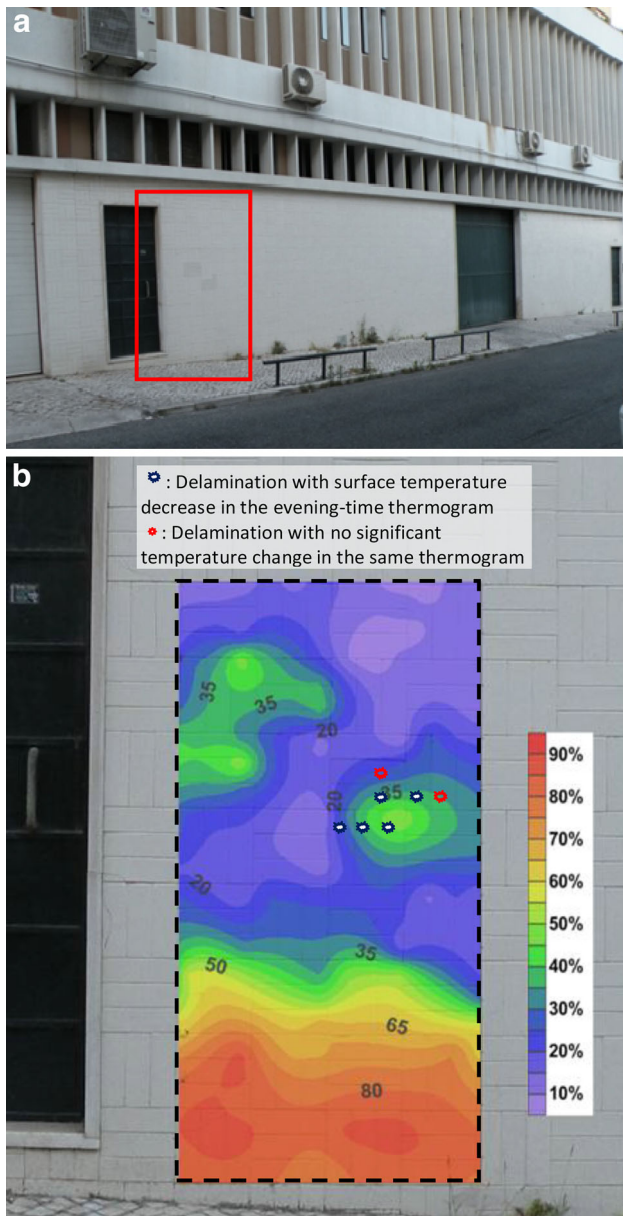


**Fig. 7** a General photograph of the west façade of B-16 showing area of interest [5], and b photograph of area of interest showing tiles with delamination on relative moisture content map

in that area can be assumed to be equal or smaller than 1 cm. In areas with delamination but without significant surface temperature change in the thermograms, the reason can be assumed to be the same as in building B-16, i.e. increased depth and/or decreased thickness of the air gap.

### 5 Discussion of the Findings of the Study

In the study, tapping control and surface moisture measurements were used as alternative in situ inspection techniques

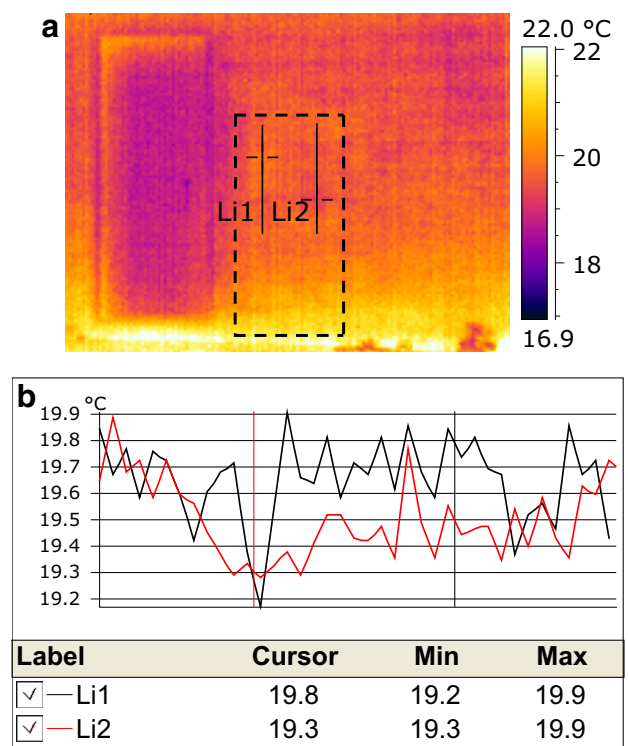


**Fig. 8** a Thermogram of the area taken during inspection IR1 [5], and b its temperature profile

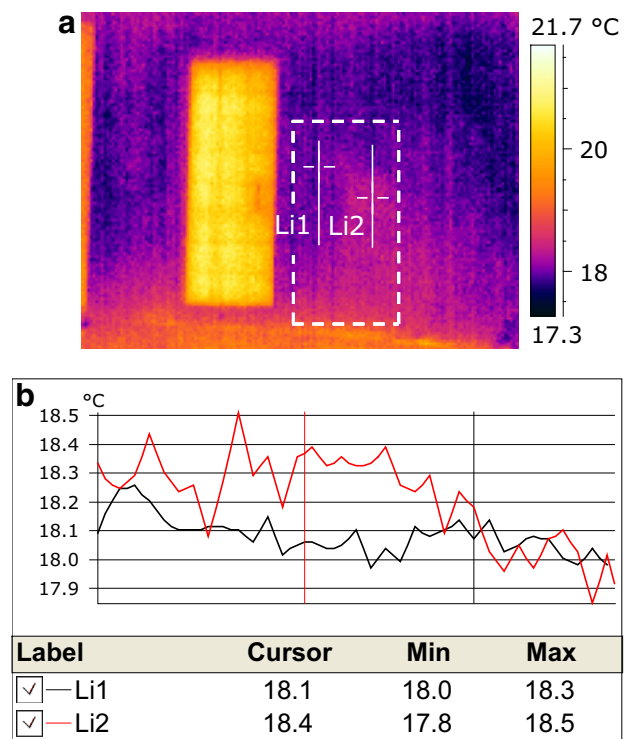


**Fig. 9** a Thermogram of the area taken during inspection IR2 [5], and b its temperature profile



**Fig. 10** Photograph of building B-11's south facade and areas of interest

to evaluate the potential of passive IRT using convective and solar heat gain to detect delamination problems of adhered ceramic claddings. Both of these techniques have some limitations. Tapping control depends on the experience of the user, and the depth and thickness of the delamination cannot be estimated. Even the identification of new defective areas, which were not noticed during the initial tapping control, was also reported by the use of alternative techniques (e.g. IRT) [31]. Capacitive type surface moisture measuring devices, such as the one used in this study, are affected by factors such as the presence of salt, metal or magnetic materials or material discontinuities that may cause errors in readings. In addition, only relative moisture measurements can be made, unless the equipment is specifically calibrated for each material [32]. However, the comparison of their results with the in situ IRT results can be said to provide sufficient evidence on the reliability/accuracy of the thermographic findings.

Numerical simulations were also performed within the context of the study to understand the thermal behaviour of sound and defective areas, and to verify the in situ IRT observations. However, the unconditioned interior environment was not accurately simulated, and the change in the amount of solar load according to the orientations was ignored. In addition, the air gap formed by delamination was modelled as an enclosed air space, where conductive heat transfer was considered only. In spite of these limitations, the results of simulations were found to be in line with the results of experimental studies given in the literature. Therefore, these simulation results together with the results of the aforementioned in situ techniques can be said to provide sufficient information to evaluate the potential of using passive IRT for the detection of delamination problems of adhered ceramic claddings.

Comparative assessment of all results showed that, in building thermography applications, passive IRT using

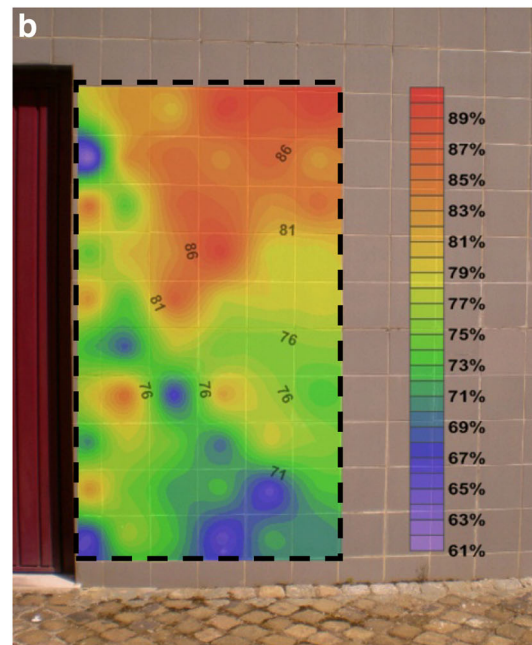
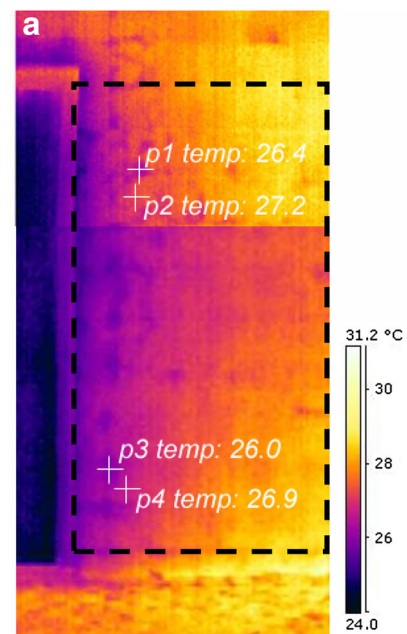


**Fig. 11** Area A: **a** merged thermogram by using the same settings; **b** photograph showing the relative moisture content map

convective and/or solar heat gain has potential, and can be used in the detection of delamination problems of adhered ceramic claddings, as 70–78 % of defective areas were identified. However, as observed in the inspections of building B-16 and area B of building B-11, some tiles with delamination may not show any significant surface temperature variation most likely due to increased depth and/or decreased thickness of the air gap. Additionally, as observed in the inspection of area A of building B-11, surface temperature variations similar to that of a delamination problem may be



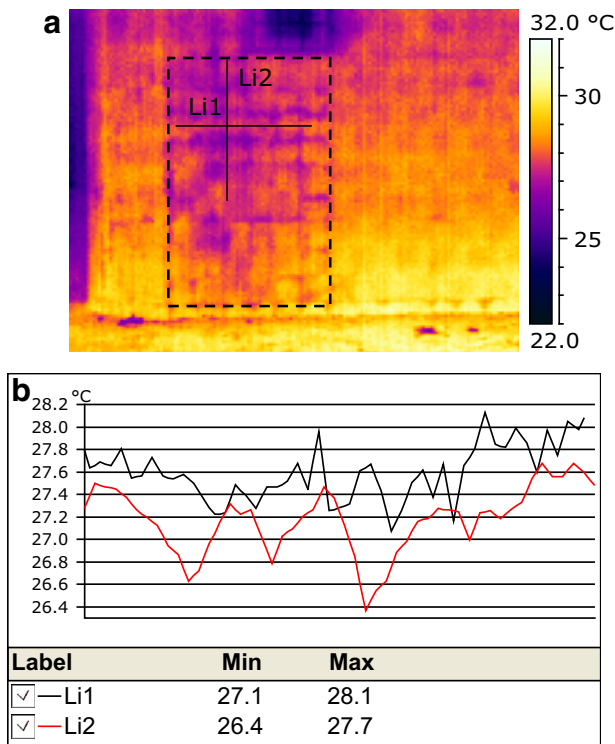


Fig. 12 a Thermogram of area B, and b its temperature profile

observed in tiles without any sign of delamination according to tapping control. Therefore, passive IRT needs to be considered as a preliminary inspection technique, like surface moisture measurement or tapping control. When possible signs of delamination are observed, more advanced techniques (usually requiring access to the facade and close-contact) such as IRT using artificial heat sources or pull-off test should be used to gather more accurate data to evaluate the presence and severity of the delamination problem. Additionally, as observed in the inspection of B-16, the moisture content increase may generate similar thermal indications such as delamination during the morning time inspections. Therefore, depending on the time of IRT inspection, performing supplementary IRT inspections might be necessary in some cases in order to determine the type of defect.

Both in situ IRT inspections and numerical thermal simulations showed that temperature variations caused by delamination are low in general. In IRT, various factors such as reflections, emissivity change due to viewing angle or thermal noise of the imaging system affect the temperature measurement, and may produce false/questionable indications similar to the ones caused by the delamination. Therefore, the selection of an IR imaging system with appropriate characteristics (e.g. low NETD), and a careful IRT inspection (e.g. viewing from different positions for determining reflections, if any) and interpretation can be said to become important.

Numerical thermal simulations showed that solar heat gain increases the surface temperature difference between sound

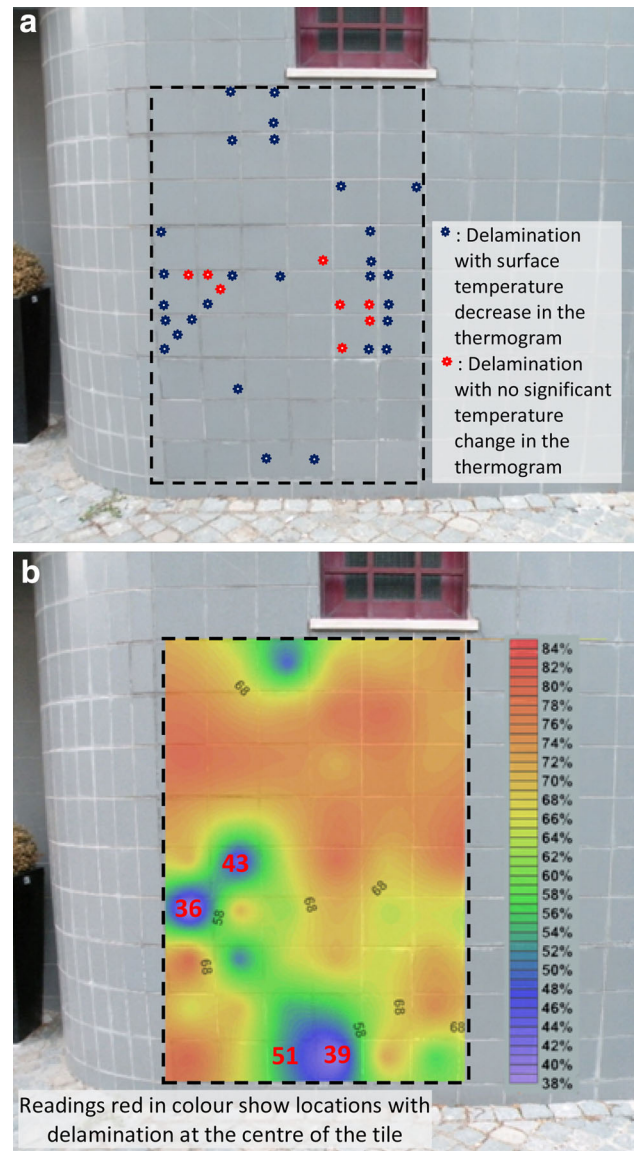


Fig. 13 Area B: a results of tapping control; b photograph showing the relative moisture content map

and defective areas both for daytime and night-time inspections. Therefore, performing IRT inspections during or after solar heat gain can be said to increase the visibility of thermal indications at the defective areas. The increased difference between exterior and interior air temperatures also increases the surface temperature difference observed in daytime conditions. Therefore, in the lack of solar heat gain due to orientation or shading, performing a daytime IRT inspection when there were large difference between interior and exterior air temperatures can be said to increase the visibility of thermal indications.

Numerical simulations also showed that maximum or minimum  $\Delta T_{[es-ed]}$  does not occur when  $T_{ed}$  or  $T_{es}$  reached to their maximum or minimum. A time-lag is created while

reaching thermal balance between sound and defective areas. Therefore, performing numerical simulations prior to IRT inspections can be said to be a guide in determining the appropriate inspection time, and also in evaluating the thermal indications observed during IRT inspection. Additionally, it can be said in general that inspection conditions (i.e. the presence and size of solar heat gain and the extent of air temperature difference) should be carefully evaluated prior to the in situ inspections to determine the appropriate timing when higher surface temperature variations can be observed.

## 6 Conclusions and Future Research

Detachment of tiles is one of the mostly seen durability problems in adhered ceramic façade claddings, which also causes safety risks. IRT has the potential to remotely detect delamination before detachment occurs. In the inspection of middle to high-rise buildings envelope, the use of natural (boundary) conditions rather than the use of artificial heat sources allows benefiting from the remote character of IRT although it is qualitative by nature. Therefore, a field research study was organised to determine the potential of passive IRT using solar and convective heat gain to detect delamination problems in adhered ceramic claddings. In two of the 16 buildings inspected in this respect, where there was access to the ceramic cladding, delamination was also confirmed by tapping control as an alternative in situ technique. 3D transient thermal simulations were also performed afterwards, using a generic wall model and considering the external environmental conditions of in situ inspection dates. The following conclusions are drawn by the comparative assessment of all findings:

- Passive IRT using solar and/or convective heat gain has the potential to detect delamination in adhered ceramic claddings. However, as the size and thickness of the air gap formed by the delamination decreases, and in relation with other conditions such as amount of heat gain, some of the areas with delamination may not give any thermographic indication. In addition, factors such as change in the compactness of grout/adhesive mortar may generate false thermographic indications in areas without delamination. Therefore, passive IRT should only be used as a preliminary inspection technique (in conjunction with other expedient techniques), and other advanced techniques such as IRT using artificial heat sources or local quantitative assessment by pull-off tests should be applied to determine the exact size and severity of the problem before deciding on any maintenance actions;
- Solar heat gain during or previous to the IRT inspection increases the surface temperature variation observed between sound and defective areas. However, the reflec-

tion of sunbeams should be considered as a potential cause of false indications in daytime inspections, especially in the inspection of glazed ceramic tiles;

- For daytime inspections, the higher the difference between exterior and interior air temperatures, the higher the surface temperature variation observed between sound and defective areas. The opposite occurs in night-time inspections. When there is lack of solar heat gain, the difference between exterior and interior air temperature can be used as a driving force creating surface temperature variations in the defective areas;
- During most of the heating period, a defective area with delamination has higher surface temperature than sound areas, and the opposite occurs during most of the cooling period. However, the time required to reach a thermal balance between sound and defective areas within the wall creates a time-lag between the transition time to and from the heating period, and the transition time to and from higher surface temperature at the defective area. Therefore, performing numerical simulations prior to the in situ IRT inspections will be a guide both to determine the timing of inspections, and to interpret and assess thermographic indications;
- Surface temperature variations observed at the defective areas will be low, and thus the precision of the surface temperature measurement becomes important. Therefore, while selecting the IR imaging device, performing the inspection and interpreting the results, special care will be necessary to guarantee the reliability of the results;
- Surface temperature variations occurring at the interior surface of the wall restrict the performance of interior IRT inspection using solar and/or convective heat gain.

The findings and conclusions of this research study can be helpful for practical application of passive IRT in the inspection of adhered ceramic claddings applied on brick walls without thermal insulation in terms of interpreting and assessing IRT indications, determining inspection time, and identifying possible sources of false IRT indications. They can also be adapted for use in the inspection of other claddings such as rendering or stone plates considering their particular characteristics, such as reflection or efflorescence, which may affect the application of passive IRT. However, since the components of the wall assembly, e.g. the presence of thermal insulation, may change the thermal response of external walls under solar and convective heat gain, further in situ IRT research coupled with numerical simulations on different wall assemblies clad with adhered ceramic tiles will be beneficial to determine changes in the IRT indications and the limits of its application. In addition, as the ambient thermal conditions also affect the thermal response of external walls, further research studies on the application of passive IRT at differing ambient thermal conditions, especially different

from the climatic conditions of Lisbon, will be beneficial to determine the potential and limits of passive IRT.

**Acknowledgments** The authors thank the Building Physics group of DECivil-IST for the technical support and for allowing the use of IR equipment. The first author thanks DECivil-IST, ICIST Research Institute, ITU, and TUBITAK for the support provided for the research visit. The other authors thank the support of the ICIST Research Institute, IST, Technical University of Lisbon and FCT (Foundation for Science and Technology).

## References

- Paiva, J.V., Aguiar, J., Pinho, A. (eds.): Guia Técnico de reabilitação habitacional (Technical guide of housing rehabilitation- vol. 2). National Institute of Habitation—Laboratory of Civil Engineering (LNEC), Lisbon (2006)
- Silvestre, J.D., de Brito, J.: Ceramic tiling in building façades: inspection and pathological characterization using an expert system. *Constr. Build. Mater.* **25**(4), 1560–1571 (2011)
- ASTM (2007) ASTM D 4788—Standard test method for detecting delamination in bridge decks using infrared thermography. American Society for Testing and Materials (ASTM) International, West Conshohocken (2007)
- Edis, E., de Brito, J., Flores-Colen, I.: Diagnosis of exterior wall failures by in situ inspection techniques—Inspection of facades with adhered ceramic cladding (Final report) (DTC No. 18/2011). Technical University of Lisbon—Institute of Engineering of Structures, Soil and Construction (UTL-ICIST), Lisbon (2011)
- Edis, E., Flores-Colen, I., de Brito, J.: Passive thermographic detection of moisture problems in facades with adhered ceramic cladding. *Constr. Build. Mater.* **51**(1), 187–197 (2014)
- Valluzzi, M.R., Grinzato, E., Pellegrino, C., Modena, C.: IR thermography for interface analysis of FRP laminates externally bonded to RC beams. *Mater. Struct.* **42**(1), 25–34 (2009)
- Tavukcuoglu, A., Akevren, S., Grinzato, E.: In situ examination of structural cracks at historic masonry structures by quantitative infrared thermography and ultrasonic testing. *J. Mod. Opt.* **57**(18), 1779–1789 (2010)
- Cerdeira, F., Vazquez, M.E., Collazo, J., Granada, E.: Applicability of infrared thermography to the study of the behaviour of stone panels as building envelopes. *Energy Build.* **43**(8), 1845–1851 (2011)
- Ghosh, K.K., Karbhari, V.M.: Use of infrared thermography for quantitative non-destructive evaluation in FRP strengthened bridge systems. *Mater. Struct.* **44**(1), 169–185 (2011)
- Lai, W.L., Lee, K.K., Kou, S.C., Poon, C.S., Tsang, W.F.: A study of full-field debond behaviour and durability of CFRP-concrete composite beams by pulsed infrared thermography (IRT). *NDT&E Int.* **52**(1), 112–121 (2012)
- Li, Z., Yao, W., Lee, S., Lee, C., Yang, Z.: Application of infrared thermography in building finish evaluation. *J. Nondestruct. Eval.* **19**(1), 11–19 (2000)
- Meola, C., di Maio, R., Roberti, N., Carlomagno, G.M.: Application of infrared thermography and geophysical methods for defect detection in architectural structures. *Eng. Fail Anal.* **12**(6), 875–892 (2005)
- Edis, E., Flores-Colen, I., de Brito, J.: Passive thermographic inspection of adhered ceramic claddings: limitations and conditioning factors. *J. Perform. Construct. Facil.* **27**(6), 737–747 (2012)
- ASTM (2010) ASTM C 1153—Standard practice for location of wet insulation in roofing systems using infrared imaging. American Society for Testing and Materials (ASTM) International, West Conshohocken (2010)
- Maldague, X.P.V.: *Nondestructive Evaluation of Materials by Infrared Thermography*. Springer, London (1992)
- Grinzato, E., Bison, P.G., Marinetti, S.: Monitoring of ancient buildings by the thermal method. *J. Cult. Herit.* **3**(1), 21–29 (2002)
- Grinzato, E., Vavilov, V., Kauppinen, T.: Quantitative infrared thermography in buildings. *Energy Build.* **29**(1), 1–9 (1998)
- Santos, C.P., Matias, L., Magalhães, A.C., Veiga, M.R.: Application of thermography and ultra-sounds for wall anomalies diagnosis. A laboratory research study. In: *Proceedings of the International Symposium—Non-Destructive Testing in Civil Engineering*, Berlin (2003). <http://www.ndt.net/article/ndtce03/papers/v082/v082.htm>. Accessed November 2013
- Maierhofer, Ch., Brink, A., Röllig, M., Wiggenhauser, H.: Transient thermography for structural investigation of concrete and composites in the near surface region. *Infrared Phys. Technol.* **43**(3–5), 271–278 (2002)
- Hung, Y.Y., Chen, Y.S., Ng, S.P., Liu, L., Huang, Y.H., Luk, B.L., Ip, R.W.L., Wu, C.M.L., Chung, P.S.: Review and comparison of shearography and active thermography for non-destructive evaluation. *Mater. Sci. Eng.* **64**(5–6), 73–112 (2009)
- Chew, M.L.: Assessing building facades using infra-red thermography. *Struct. Surv.* **16**(2), 81–86 (1998)
- Washer, G., Fenwick, R., Bolleni, N.: Effects of solar loading on infrared imaging of subsurface features in concrete. *J. Bridge Eng.* **15**, 384–390 (2010). Special Issue: Bridge Inspection and Evaluation
- ANSYS (2010) ANSYS Release 13.0—ANSYS FLUENT theory guide. ANSYS Inc., Canonsburg (2010)
- Dos Santos, C.A.P., Matias, L.: Coeficientes de transmissão térmica de elementos da envolvente dos edifícios [Heat transfer coefficients of the envelope elements of buildings] (ICT Technical Information, Buildings-ITE 50). National Laboratory of Civil Engineering (LNEC), Lisbon (2006)
- BSI: BS EN 12524:2000 Building materials and products—Hygrothermal properties—Tabulated design values. British Standards Institution, London (2000)
- IPQ (2006). NP EN 1745: 2005 Alvenarias e elementos de alvenaria. Métodos para determinação de valores térmicos de cálculo [NP EN 1745: 2005 Masonry and masonry products. Methods for determining design thermal values]. Caparica: Portuguese Quality Institute (IPQ) (2006).
- DOE (2011) EnergyPlus Simulation Software: Weather Data. US Department of Energy (2011). [http://apps1.eere.energy.gov/buildings/energyplus/cfm/weather\\_data3.cfm/region=6\\_europe\\_wmo\\_region\\_6/country=PRT/cname=Portugal](http://apps1.eere.energy.gov/buildings/energyplus/cfm/weather_data3.cfm/region=6_europe_wmo_region_6/country=PRT/cname=Portugal). Accessed June 2012
- ANSYS (2010) ANSYS Release 13.0—ANSYS FLUENT user's guide. ANSYS Inc., Canonsburg (2010)
- RCCTE: Regulamento das Características de Comportamento Térmico dos Edifícios [Regulation of the Thermal Behaviour Characteristics in Buildings]. *Diary of Republic I series-A*, **67**, 2468–2513 (2006)
- ASTM (2003) ASTM-C 1060–90 Standard practice for thermographic inspection of insulation installations in envelope cavities of frame buildings. American Society for Testing and Materials (ASTM) International, West Conshohocken (2003).
- Clark, M.R., McCann, D.M., Forde, M.: Application of infrared thermography to the non-destructive testing of concrete and masonry bridges. *NDT&E Int.* **36**(4), 265–275 (2003)
- Phillipson, M.C., Baker, P.H., Davies, M., Ye, Z., McNaughtan, A., Galbraith, G.H., McLean, R.C.: Moisture measurement in building materials: an overview of current methods and new approaches. *Build. Serv. Eng. Res. Tech.* **28**(4), 303–316 (2007)